Hindawi
Geofluids
Volume 2019, Article ID 2985691, 12 pages
https://doi.org/10.1155/2019/2985691

Research Article

Damage and Failure Evolution Mechanism for Coal Pillar Dams Affected by Water Immersion in Underground Reservoirs

Fangtian Wang[1,2] **Ningning Liang**[3] **and Gang Li**[1]

[1]*School of Mines, State Key Laboratory of Coal Resources and Mine Safety, Key Laboratory of Deep Coal Resource Mining, Ministry of Education of China, China University of Mining and Technology, Xuzhou, Jiangsu 221116, China*
[2]*State Key Laboratory of Groundwater Protection and Utilization by Coal Mining, Beijing 100011, China*
[3]*DADI Engineering Development Co. Ltd., Beijing 100102, China*

Correspondence should be addressed to Ningning Liang; liangning@cumt.edu.cn

Received 28 June 2018; Revised 11 October 2018; Accepted 26 October 2018; Published 6 January 2019

Academic Editor: Stefano Lo Russo

In coal mines, underground reservoir systems can increase the availability of water and are an effective technical approach for the protection and utilization of water resources. The stability of coal pillar dams is the key factor in the safety and stability of these underground water storage systems. However, coal pillar dams must operate in complex environments that combine dynamic-static superimposed stress fields and water immersion; moreover, coal pillar dams subjected to both stress and seepage are more susceptible to damage and even collapse. In this study, a seepage-stress coupling model of a coal pillar dam was constructed using the Universal Distinct Element Code (UDEC) simulation software. This model provides a platform for analyzing the characteristics of fracture development in surrounding rock in active mines and the coupled development of crack fields and seepage fields in coal pillar dams. Methods were developed for (1) calculating the water content for the coal pillar dam numerical simulation model and (2) reducing water immersion weakening. The maximum seepage width of a coal pillar dam subjected to water immersion was obtained, and a damage and failure evolution mechanism for coal pillar dams experiencing flooding was developed. The results provide a scientific basis for enhancing the stability control of coal pillar dams and are of great significance for realizing water conservation in coal mines.

1. Introduction

The protection and utilization of water resources are a major challenge in the green mining of coal [1]. High-intensity mining can have a significant environmental impact, and the negative environmental effects caused by coal mining are becoming more prominent [2]. At the same time, the construction of mining areas brings difficulties such as water acquisition, comprehensive utilization of water resources, and water rights allocation [3–5]. Therefore, coordinating coal mining and the protection and utilization of water resources are a key issue in the green mining of coal, particularly in arid and semiarid areas, where water resources are scarce and the surface ecology is fragile (e.g., the coal-rich regions of western China).

The mining of coal seams leads to breakages and movement in the overlying strata, which changes the distribution of groundwater flow fields. A groundwater funnel with a goaf as the gathering area and a water flowing fractured zone as the center of seepage are formed, causing excessive loss of ground and surface water; this can cause environmental damage such as the death of vegetation and the intensification of desertification [6, 7], as shown in Figure 1.

Storing water in underground goafs, connecting coal pillars with artificial dams, and constructing mine water storage and water intake facilities allow for the development of underground reservoir systems which represent an effective means of protecting and utilizing water resources in coal mines. Where a goaf space is very large and pores and fissures are extremely developed, the underground goaf can be used

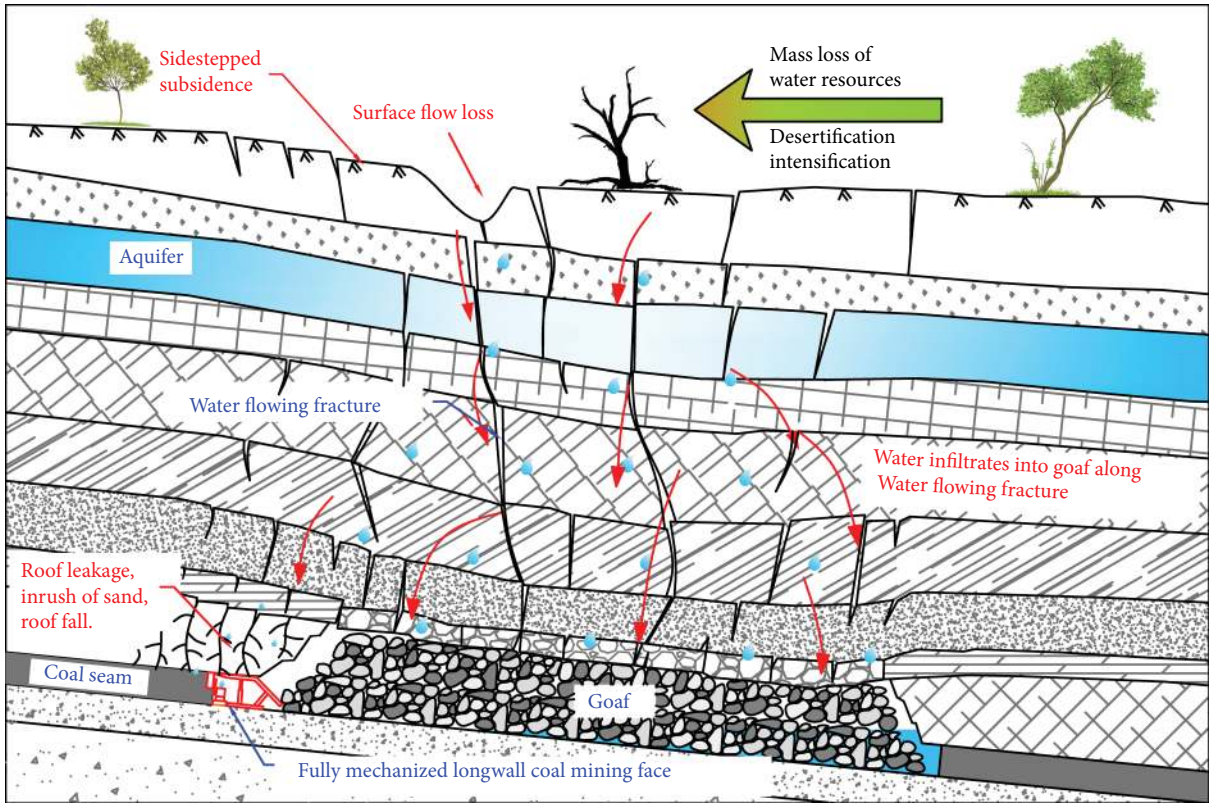

Figure 1: Water environmental damage processes and pathways triggered by longwall mining.

to store water, thus increasing the total water resources available in the mine area [8]. Moreover, when a large number of granule particles remain in the goaf, they provide the ability to absorb pollution by effectively removing suspended particles and colloid materials from the mine water [9, 10]. This purified mine water can be used for tasks such as dust reduction, coal washing, and irrigation.

Scholars have conducted extensive research into engineering practices that improve the protection and utilization of coal mine water resources. Outside of China, mine water discharged from the coal mining process is generally regarded as a valuable water resource. Typically, large-flow, high-head pumps are used to forcibly drain the aquifers of the main coal seam and mine water that has not been polluted by mining is discharged directly into the ground, resulting in a high mine water utilization rate. For example, in the 1980s, the utilization rate of coal mine water in the United States was 81%; in 1995, the utilization rate of coal mine water at Donbass mine, Ukraine, exceeded 90% [11–13]. India and Japan have established underground reservoirs for storing groundwater using rock formations [14, 15]; these have been generally formed by intercepting and storing groundwater using a water-intercepting wall; however, the cost is relatively high. Poland has proposed the use of goafs to store water resources, and the suitability of abandoned mines for water storage in goafs, wells, and mining fissures has been considered. However, permanently sealing underground spaces is costly, particularly in the case of deep mines, and as a result, no further research has been conducted and practical uses have not been established [16]. Although the idea of using goafs for water storage and reuse has been proposed, no complete technical system of underground reservoir construction has been established and practical verification is lacking.

After the impoundment of underground reservoirs, coal pillar dams become complex environments in which both a dynamic-static superimposed stress field and water immersion coexist; mechanical parameters such as the strength, elastic modulus, and cohesion of the coal subjected to water immersion can change significantly. A coal pillar dam under the coupling of stress and seepage is more susceptible to damage and even collapse. To study the damage and fracture mechanisms of coal pillar dams immersed in water, this study employed UDEC (Universal Distinct Element Code) to establish a numerical calculation model on the basis of the geological conditions and operational state of an underground reservoir. We examined (1) the characteristics of fracture development in surrounding rock influenced by a complex stress field, (2) the evolution of fracture fields and seepage fields in coal pillar dams, and (3) the damage and failure mechanisms of a coal pillar dam immersed in water. The study addresses the urgent need for construction of underground reservoirs, while considering long-term operational safety and important scientific issues related to energy development and environmental protection. Our findings provide a scientific basis for realizing the long-term safe operation of coal mine groundwater reservoir systems.

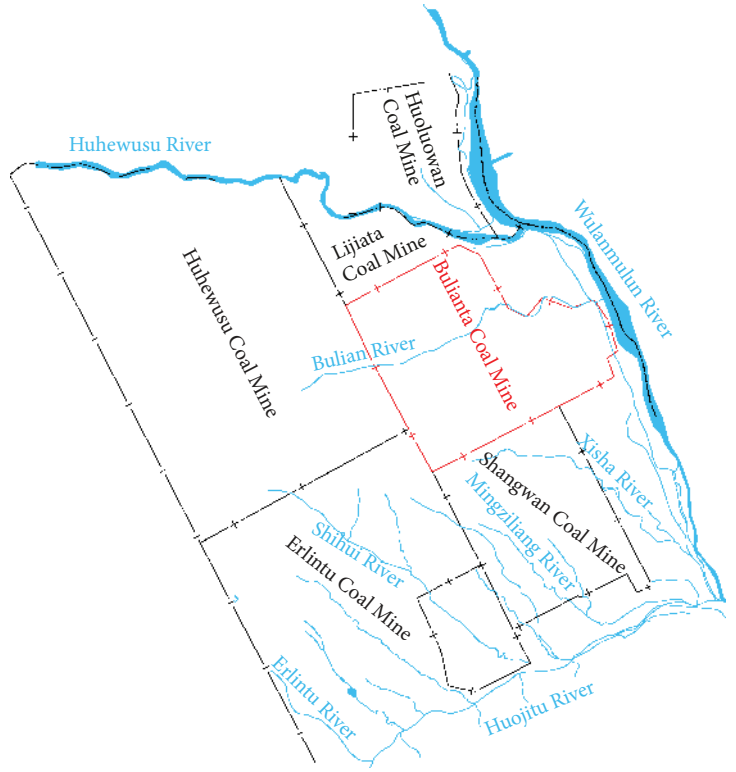

Figure 2: Schematic diagram of the surface water system in the area around the Bulianta Coal Mine.

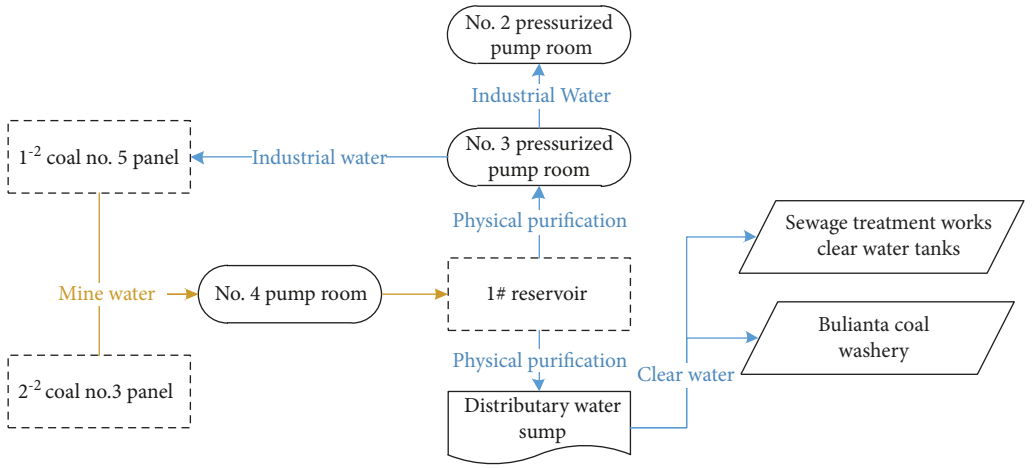

Figure 3: Supply and drainage system diagram of the #1 reservoir in the Bulianta Coal Mine.

2. Engineering Background

The Bulianta Coal Mine is located in the China Shendong Mining Area, which has a shortage of water resources and a fragile ecological environment. The surface water system in the mining area is relatively developed, as shown in Figure 2. The Huhewusu, Bulian, and Huojitu rivers are perennial surface waters, while other rivers are seasonal streams. The mean annual rainfall in the mining area is 396 mm and the mean annual evaporation is 2457.4 mm; the surface water evaporation is much greater than the precipitation. The geomorphological features and geological structure of the mining area are not conducive to the formation of natural groundwater reservoirs.

The production water used in the Bulianta Coal Mine is mainly extracted from groundwater resources. In the past, the water produced by coal mining was mainly discharged onto the ground and was not properly utilized. To alleviate the shortage of mine water, an underground reservoir project was successfully implemented. The #1 reservoir is located in the goaf of the 22301–22305 working panels and is the permanent source of water for the mine. The water storage

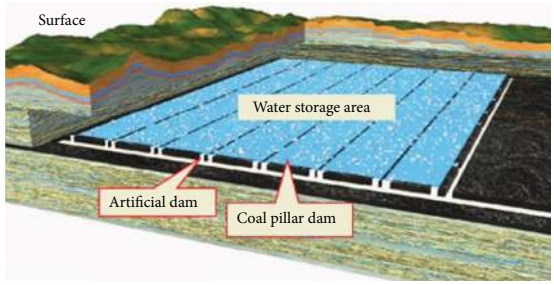

(a) Dam structure of underground reservoirs in coal mines

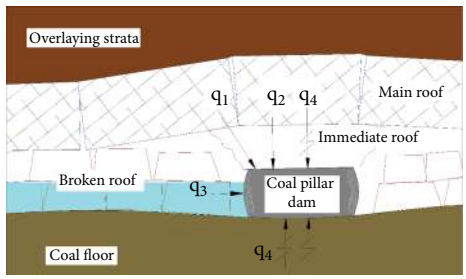

(b) Stress environment diagram of coal pillar dams

(q_1: side abutment pressure; q_2: overlying strata gravity; q_3: hydrostatic pressure; q_4: dynamic stress)

Figure 4: Structure and stress environment diagrams for coal pillar dams in underground reservoirs.

capacity is 800,000 m^3; the current water storage height is 2.4 m, and 182,000 m^3 is being stored. The water supply and drainage system are shown in Figure 3.

The reservoir dam is composed of the coal seam safety pillar and an artificially constructed dam, as shown in Figure 4(a). The stability of the coal pillar dam is a key factor in the safe and stable operation of the underground reservoir system. After a working face is mined, the rock strata collapse and stress is redistributed. As shown in Figure 4(b), the stress environment of the coal pillar dam changes from a single stress state to a complex stress environment, where stress is superimposed by the overlying rock column pressure, the bearing pressure of the stope, the lateral pressure stress from the broken roof, and microearthquakes in the mine. In the meantime, water immersion changes the mechanical response and deformation characteristics of the coal.

3. Influence of Water Immersion on Coal

3.1. Characteristics of Coal Weakened by Water Immersion. Scholars have conducted extensive research into the mechanical parameters of a coal body immersed in water. According to an experiment by Liu et al. [17], the uniaxial compressive strength (σ_{bc}) and uniaxial tensile strength (σ_t) of coal decrease with an increase in moisture content (MC). Guo [18] conducted a mechanical test by soaking coal samples and found that the uniaxial compressive strength and elastic modulus of the coal samples were nonlinearly related to the moisture content of the coal samples. Through a chamfering shear test, Niu [19] found that the cohesion (c) and internal friction angle (φ) of coal decrease with an increase in moisture content; this relationship is illustrated in Figure 5.

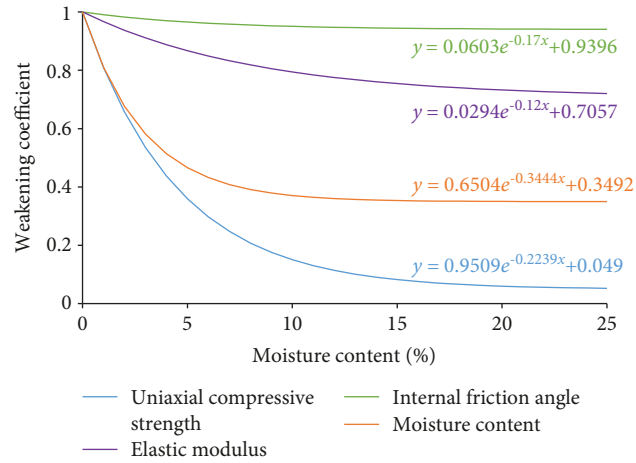

Figure 5: Relationship between weakening coefficient and moisture content in coal.

Coal strength reduction due to water immersion is known as coal weakening. The weakening coefficient (y) indicates the degree of influence of water on the coal strength weakening. Figure 5 shows that as the moisture content of the coal increases and the elastic modulus, compressive strength, cohesion, and internal friction angle of the coal are all weakened to different degrees. Among them, the degree of weakening of the compressive strength is the highest and the degree of weakening of the internal friction angle is the lowest. An increase in moisture content from 0% to 8% has a significant effect on the weakening of the elastic modulus. After the moisture content exceeds 8%, the elastic modulus coefficient remains stable. Increasing the moisture content from 0% to 15% has a more pronounced effect on the weakening of the compressive strength of the coal. When the moisture content is greater than 15%, the compressive strength of the coal sample is less than 5% of the compressive strength at a moisture content of 0%.

3.2. Numerical Inversion of Uniaxial Compression Experiments. To verify the reliability of the numerical calculation model grid partition and selected parameters for a coal pillar dam immersed in water, a UDEC uniaxial compression calculation model with a width of 50 mm and a height of 100 mm was established. The numerical calculation model consisted of 111 Voronoi blocks. The upper and lower ends of the block were rigid loading plates. The Mohr-Coulomb failure criterion was applied to the block elements. The joints adopted the Mohr-Coulomb slip surface strength criterion, and the experiments were carried out according to the velocity loading mode and stress displacement curve in the model test monitoring process. The numerical calculation model is shown in Figure 6(a), the mechanical parameters of the model are listed in Table 1, and the results generated by the model are shown in Figures 6(b), 6(c), and 7.

As shown in Figure 6(b), the center of the specimen appeared to swell under the action of rigid loading plates at both ends. The displacement of the specimen close to the loading plates at both ends was mainly in the vertical

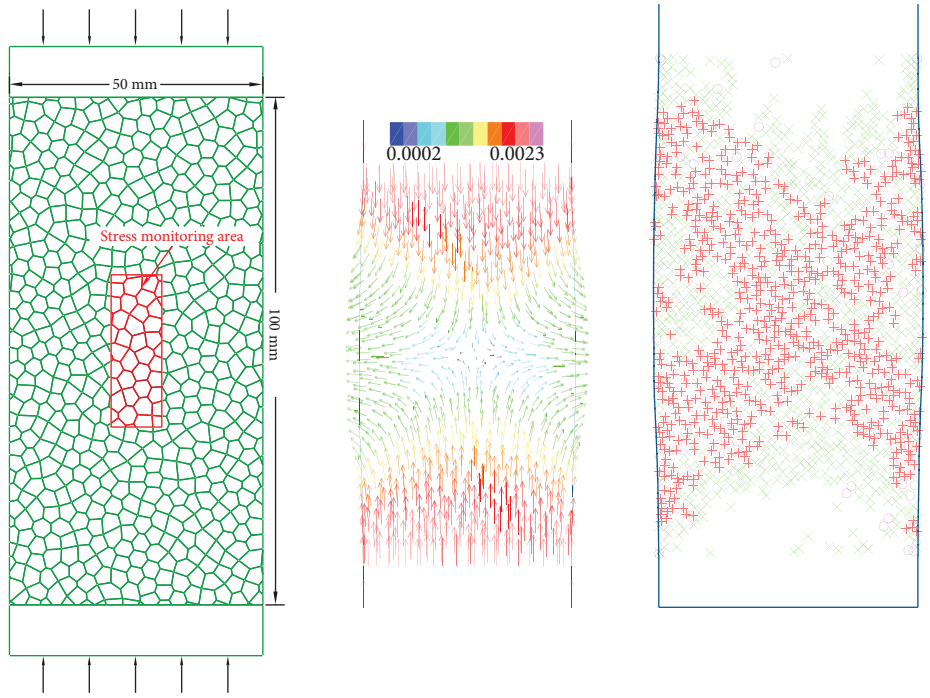

(a) Numerical model diagram (b) Displacement vector distribution (c) Plastic zone distribution

Figure 6: Numerical model and simulation result.

Table 1: Physical and mechanical properties of coal.

Volumetric weight (ρ) (kN·m^{-3})	Elastic modulus (E) (GPa)	Shear modulus (K) (MPa)	Tensile strength (σ_t) (MPa)	Cohesion (c) (MPa)	Internal friction angle (φ) (°)	Poisson ratio (μ)
15.00	14.00	3.00	0.30	1.80	25	0.22

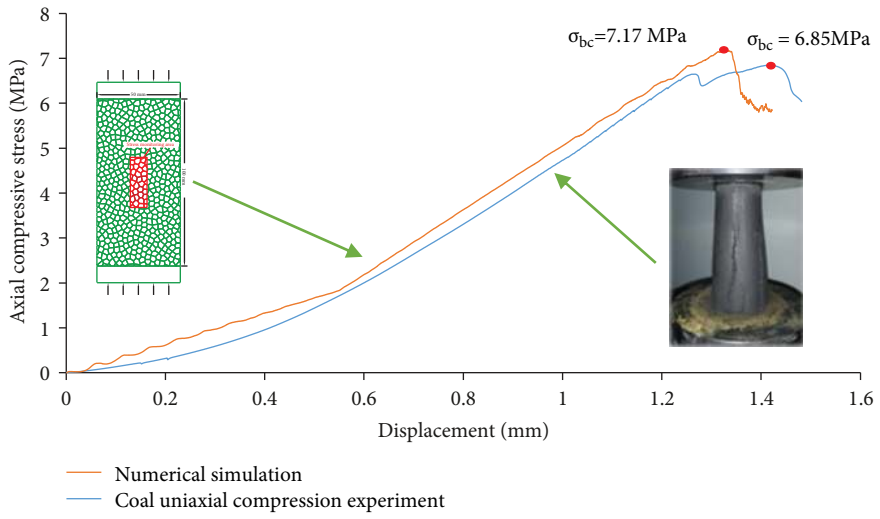

Figure 7: Uniaxial compression stress displacement curve.

direction, while the center displacement of the specimen was mainly in the horizontal direction. As shown in Figure 6(c), except for some areas near the loading plates, the specimens were in a plastic state after loading. An X-shaped conjugate bevel shear failure zone was formed in the middle of the specimen, indicating that the failure of the specimen was mainly affected by the shear stress on the displacement vector transformation surface.

As shown in Figure 7, the stress displacement curve of the UDEC numerical model is basically consistent with that

Table 2: Physical and mechanical properties of coal after weakening.

Moisture content (MC) (%)	Volumetric weight (ρ) (kN·m^{-3})	Elastic modulus (E) (GPa)	Shear modulus (K) (MPa)	Tensile strength (σ_t) (MPa)	Cohesion (c) (MPa)	Internal friction angle (φ) (°)	Poisson ratio (μ)
0	15.00	14.00	3.00	0.30	1.80	25	0.22
5	15.00	6.52	1.40	0.11	1.74	21.68	0.22

of the uniaxial compression test. The compressive strength of the UDEC simulation was 7.17 MPa, the compressive strength of the coal sample under uniaxial compression was 6.85 MPa, and the overall difference was relatively small. At this time, the mechanical parameters and grid division used in the numerical calculation model can simulate the uniaxial compression process of the coal.

To verify whether the relationship between the coal weakening coefficient and moisture content in Figure 5 is also valid in the numerical simulation, the mechanical parameters in Table 1 were substituted into the corresponding formulas, the mechanical parameter weakening coefficients were obtained when the moisture content was 5%, and the mechanical parameters were obtained after weakening, as shown in Table 2. These parameters were then used in the numerical calculations to obtain the corresponding uniaxial compression stress displacement curve, as shown in Figure 8.

According to Figure 5, the weakening coefficient of compressive strength is 0.3595 when the moisture content is 5% and the theoretical compressive strength is 2.58 MPa. Figure 8 shows that the compressive strength of the numerical model with weakened mechanical parameters was 2.26 MPa. It is considered that the correlation coefficient between the physical and mechanical properties of the coal sample and the moisture content is reliable. This indicates that numerical simulation reflects the influence of moisture content on mechanical properties.

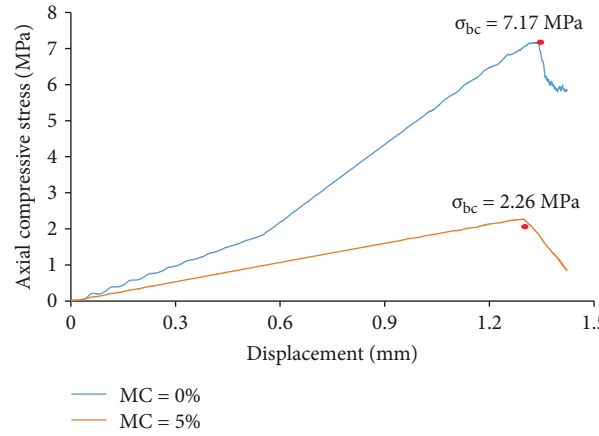

Figure 8: Uniaxial compression stress displacement curve after weakening.

4. Seepage Field Distribution Characteristics of Coal Pillar Dams

4.1. Construction of Numerical Model. To study the fracture-seepage distribution characteristics and damage evolution law of coal pillar dams immersed in water, a UDEC numerical calculation model was established on the basis of actual geological conditions. As shown in Figure 9, the model was 250 m wide and 180 m high. Divided into 12 strata, the rock strata were divided into different sizes according to the mechanical characteristics of the coal and rock mass and the calculation requirements.

The upper boundary of the numerical model adopts the free boundary condition. The left and right boundaries limit the horizontal velocity, and the lower boundary limits the vertical velocity. The Mohr-Coulomb strength criterion is adopted for the vertical model block element, and the Mohr-Coulomb strength criterion for joint surface contact is adopted. The mechanical parameters selected at various layers of the model are shown in Table 3, and the gravity acceleration is 10 m/s^2. There are 50 m protection pillars at both ends of the modulus.

Both the left and right boundaries and the lower boundary of the model were set as impervious boundaries. According to the operation of underground reservoirs, a 24 kPa head pressure was applied to the auxiliary roadway in the mined working face.

4.2. Plastic Zone Development in a Coal Pillar Dam after Mining the Face. After mining on the working face, the redistribution of stress results in plastic failure in the coal. The development of a plastic zone in the surrounding rock of the roadway is shown in Figure 10.

A half-circle-shaped plastic zone appears in the coal wall of the roadway. The plastic zone depths of the two auxiliary roadway ribs are approximately 1.64 m and 1.93 m, while the plastic zone depth of the ventilation roadway is approximately 2.77 m. Owing to the influence of roof rotation deformation, the plastic zone is formed above the roadway. Moreover, the width of the plastic zone decreases gradually as it is far away from the goaf.

4.3. Seepage Field Distribution of Coal Pillar Dams after Reservoir Impoundment. There are numerous mutually conducting and penetrating cracks in the surrounding rock of a roadway subjected to repeated mining. After being stored underground, water flows into the coal pillar dam along cracks that are under hydrostatic pressure. As shown in Figure 11, the distribution of seepage pressure in the coal pillar dam is triangular and the maximum penetration width is about 6.56 m. There are also numerous penetrating cracks in the coal floor, which is subjected to repeated mining. The maximum infiltration width in the floor is about 8.48 m, and the maximum infiltration depth is about 4 m.

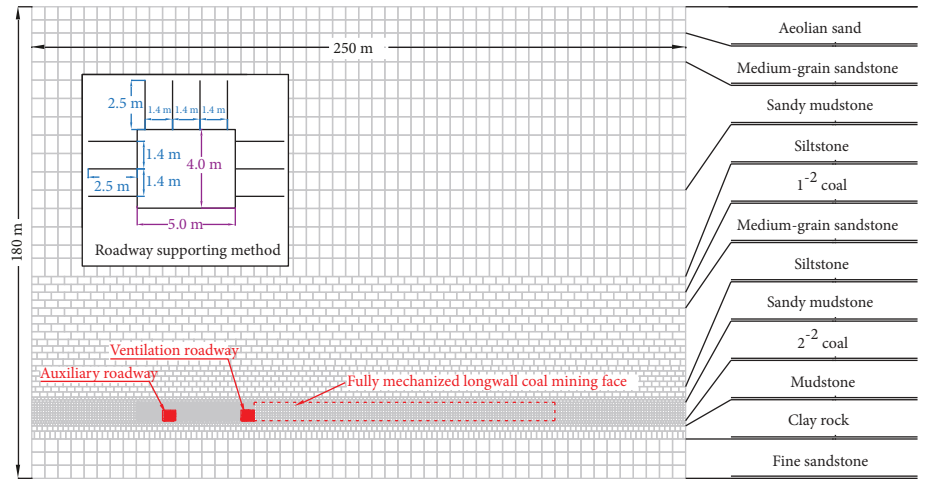

Figure 9: Schematic diagram of numerical calculation for seepage and fracture of a coal pillar.

Table 3: Physical and mechanical properties of coal and rock.

Lithology	Thickness (m)	Volumetric weight (ρ) (kN·m^{-3})	Elastic modulus (E) (GPa)	Compressive strength (σ_{bc}) (MPa)	Poisson ratio (μ)
Aeolian sand	10	15.8	—	—	—
Medium-grain sandstone	11	23.9	33	45.3	0.25
Sandy mudstone	49	22.4	23	22.8	0.28
Siltstone	33	23.5	35	40.6	0.25
1^{-2} coal	6	14.8	15	6.6	0.35
Medium-grain sandstone	11	23.9	33	45.3	0.25
Siltstone	30	23.5	35	40.6	0.25
Sandy mudstone	6	22.4	23	22.8	0.28
2^{-2} coal	7	15.1	14	6.6	0.22
Mudstone	2	22.3	20	20.7	0.3
Clay rock	5	20.4	35	19.6	0.28
Fine sandstone	15	23.4	13	6.6	0.22

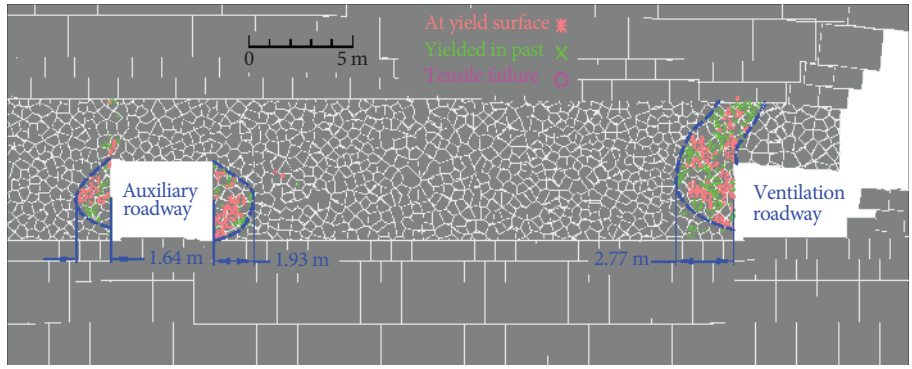

Figure 10: Distribution map of the plastic zone of the coal pillar.

5. Damage Evolution of the Coal Pillar Subjected to Water Weakening

After impoundment of an underground reservoir, the cracks in the coal pillar dam are filled with water. Water has physical and chemical effects on coal, including lubrication, weakening, and slime. Water weakening of coal is one of the main reasons for coal damage after water immersion, as water immersion will aggravate the damage and deterioration of coal. A numerical simulation that does not consider the effect of water immersion on the weakening of coal can only reflect how changes in the stress environment cause damage and deterioration in coal. To study the damage and deterioration characteristics of a coal pillar dam subjected to water

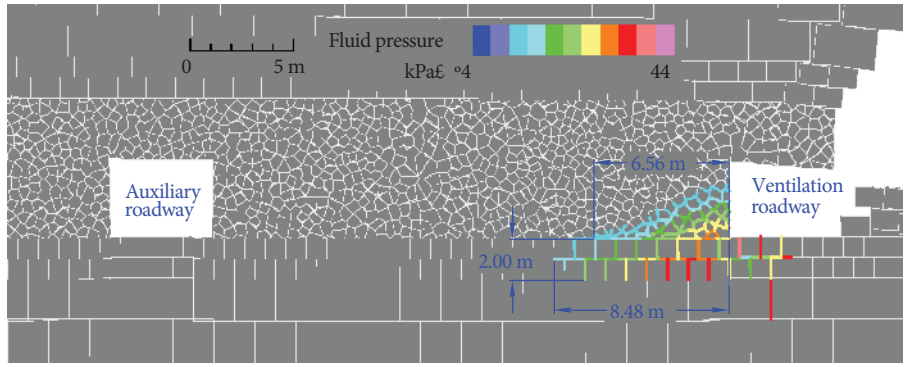

Figure 11: Distribution map of the seepage field of the coal pillar.

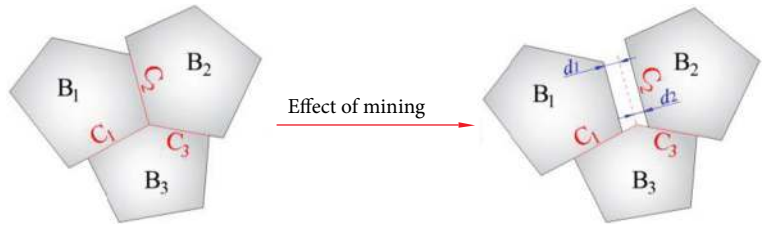

Figure 12: Representation of moisture content method.

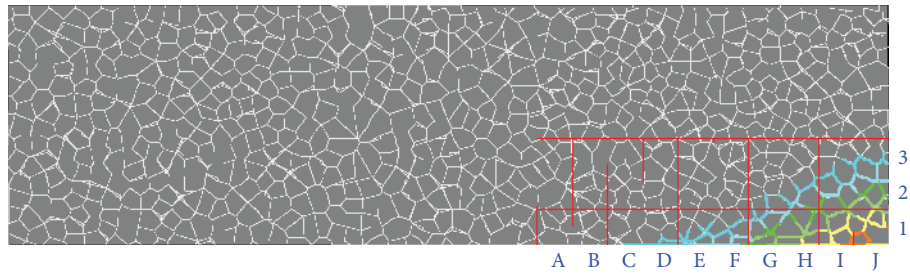

Figure 13: Schematic diagram of processing unit division.

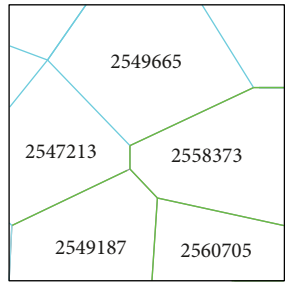

Figure 14: Schematic diagram of the F1 processing unit.

weakening, the relationship between the mechanical parameters of the coal body and the moisture content in Figure 5 should be entered into the numerical calculation model. Simulation results obtained in this manner can be used to approximately characterize the damage evolution of coal pillar dams subjected to water immersion.

5.1. Representation Method of Moisture Content in Numerical Calculation. The UDEC numerical simulation model consists of block and contact units. In the process of software operation, a block will model rotations, displacements, and deformations as the stress environment changes, while a contact models slips and opens. A contact in the open state forms a seepage channel for the liquid in the numerical simulation. On the basis of not considering the possible chemical action of coal and fluid and assuming that coal and fluid are incompressible and the density is invariable, this paper suggested that the cavity formed by moving block will be filled with fluid under the influence of seepage pressure and no fluid will flow into the cavity without seepage pressure. And that means that the moisture content of the processing unit is related to the distribution range of seepage pressure and the opening of contact between the blocks, as shown in Figure 12.

It can be seen from Figure 12 that as the result of mining action, the block has been displaced. The normal displacement of block B_1 relative to the initial position is d_1, the normal displacement of block B_2 relative to the initial position is d_2, and the contact length is l. The area of the space formed by the block displacement at this time is $l \times (d_1 + d_2)$. In this case, if in contact with nonzero seepage pressure, it can be considered that the cavity formed by the contact opening is filled with fluid. Then the volume of cavity can

Table 4: Block and contact information of the F1 processing unit.

Block ID	Block area (s^2)	Contact ID	Contact length (m)	Normal displacement (mm)
2547213	0.1507	8110032	0.2194	5.0399
		2548431	0.4316	5.4270
		2548284	0.0849	0.7235
		2548607	0.4763	5.5610
		2548519	0.0134	6.9820
2535070	0.0152	8100550	0.2194	5.0288
		8104822	0.1463	6.664
2540996	0.0349	8109856	0.1463	6.661
		2541440	0.2385	2.8444
2549665	0.2356	2548343	0.4316	5.5590
		2541075	0.2385	3.5144
		2550886	0.3578	5.7025
2559699	0.0612	8091739	0.4967	9.1313
		2550844	0.3578	8.0616
		2558729	0.4967	9.5340
2558373	0.1833	2548242	0.0849	1.2428
		2551033	0.4967	7.3613
		2558494	0.4967	8.0590
		2558641	0.4707	7.3750
2560705	0.1176	2549383	0.1448	5.1230
		2558553	0.4707	6.3380
		2549471	0.3007	1.2508
2549187	0.1533	2548607	0.4763	5.5610
		2549266	0.1448	5.0460
		2549005	0.3007	2.0306
2538882	0.0010	2540361	0.2002	0.8095
		2540420	0.0134	6.3420
		2540319	0.2002	0.8101
$\sum V$	0.9528	$\sum ld$	0.0472	

be approximately equivalent to the volume of the fluid, and the moisture content in the numerical model can be expressed as

$$\eta = \frac{\rho_1(ld_1 + ld_2)}{\rho_1(ld_1 + ld_2) + \rho_2(V_{B1} + V_{B2} + V_{B3})}, \quad (1)$$

where η is the moisture content (%), ρ_1 is the fluid density, l is the contact length, d_1/d_2 is the normal displacement of the block, ρ_2 is the block density, and $V_{B1}/V_{B2}/V_{B3}$ is the block area.

To simplify data processing and improve the accuracy of moisture content in the numerical model, the coal pillar dam numerical model is divided into 1×1 m grids (Figure 13).

Each grid is treated as a processing unit, and the moisture content of the unit is obtained by data processing, taking grid F1 as an example (Figure 14).

As shown in Figure 14, the F1 processing unit consists of all or part of nine blocks and contacts. In the numerical model, the "print block ID" command is used to index the contact number corresponding to the block; the "print contact ID" command is then used to retrieve the length and normal displacement of the corresponding contact and to summarize the acquired block and contact data, as shown in Table 4.

The moisture content of the F1 processing unit can be expressed as

$$\eta_{F1} = \frac{\rho_1 \sum ld}{\rho_1 \sum ld + \rho_2 \sum V}, \quad (2)$$

where η_{F1} is the moisture content of the F1 processing unit (%), ρ_1 is the fluid density, ρ_2 is the block density, $\sum ld$ is the sum of void areas of the contact with nonzero seepage pressure in the processing unit, and $\sum V$ is the sum of block area of the F1 processing unit. After calculation, $\eta_{F1} = 4.72\%$.

It can be seen from Figure 5 that when the moisture content is 4.72%, the internal friction angle weakening coefficient is 0.8728, the cohesion weakening coefficient is 0.9667, the elastic modulus weakening coefficient is 0.4776, and the compressive strength weakening coefficient is 0.3795. The mechanical parameters of the F1 processing unit after water weakening treatment are shown in Table 5:

The numerical simulation mechanical parameters obtained through water immersion weakening are assigned to the block of the F1 processing unit. According to the same processing method, the moisture content of the other processing units was calculated separately and the mechanical parameters after weakening were determined; these are assigned to the corresponding unit blocks. The processing flow chart is shown in Figure 15. Secondary weakening treatments were carried out for processing units whose seepage field distribution changed significantly in the numerical model.

5.2. Plastic Zone Development Law of the Coal Pillar Dam Subjected to Water Weakening. The plastic zone development of the coal pillar dam is shown in Figure 16.

After weakening the mechanical parameters of the numerical model of the coal pillar, the plastic zone depths of the two auxiliary roadway ribs are 1.85 m and 2.25 m, which are 0.21 m and 0.32 m greater than their original respective preweakened states.

The depth of the plastic zone at the bottom of the ventilation roadway rib is deeper than that at the upper; the depth of the plastic zone at the bottom is about 8.25 m, which is 5.48 m greater than that before the water weakening. As they were affected by the distribution characteristics of the seepage field, the area and depth of the weakened area under the coal pillar dams are relatively large. As a result, the coal is more susceptible to plastic failure and the development of fissures is intensified; this, in turn, causes the seepage field to expand deep into the coal pillar dams.

As a result of water immersion, the strength of coal is decreased and it is more likely to become damaged and lose its bearing capacity. As a result, the stress is transferred to the deep part of the coal, which aggravates the stress environment

Table 5: Physical and mechanical properties of coal after weakening of the F1 processing unit.

Moisture content (MC) (%)	Volumetric weight (ρ) (kN·m^{-3})	Elastic modulus (E) (GPa)	Shear modulus (K) (MPa)	Tensile strength (σ_t) (MPa)	Cohesion (c) (MPa)	Internal friction angle (φ) (°)	Poisson ratio (μ)
0	15.00	14.00	3.00	0.30	1.80	25	0.22
4.72	15.00	6.69	1.43	0.11	1.74	21.82	0.22

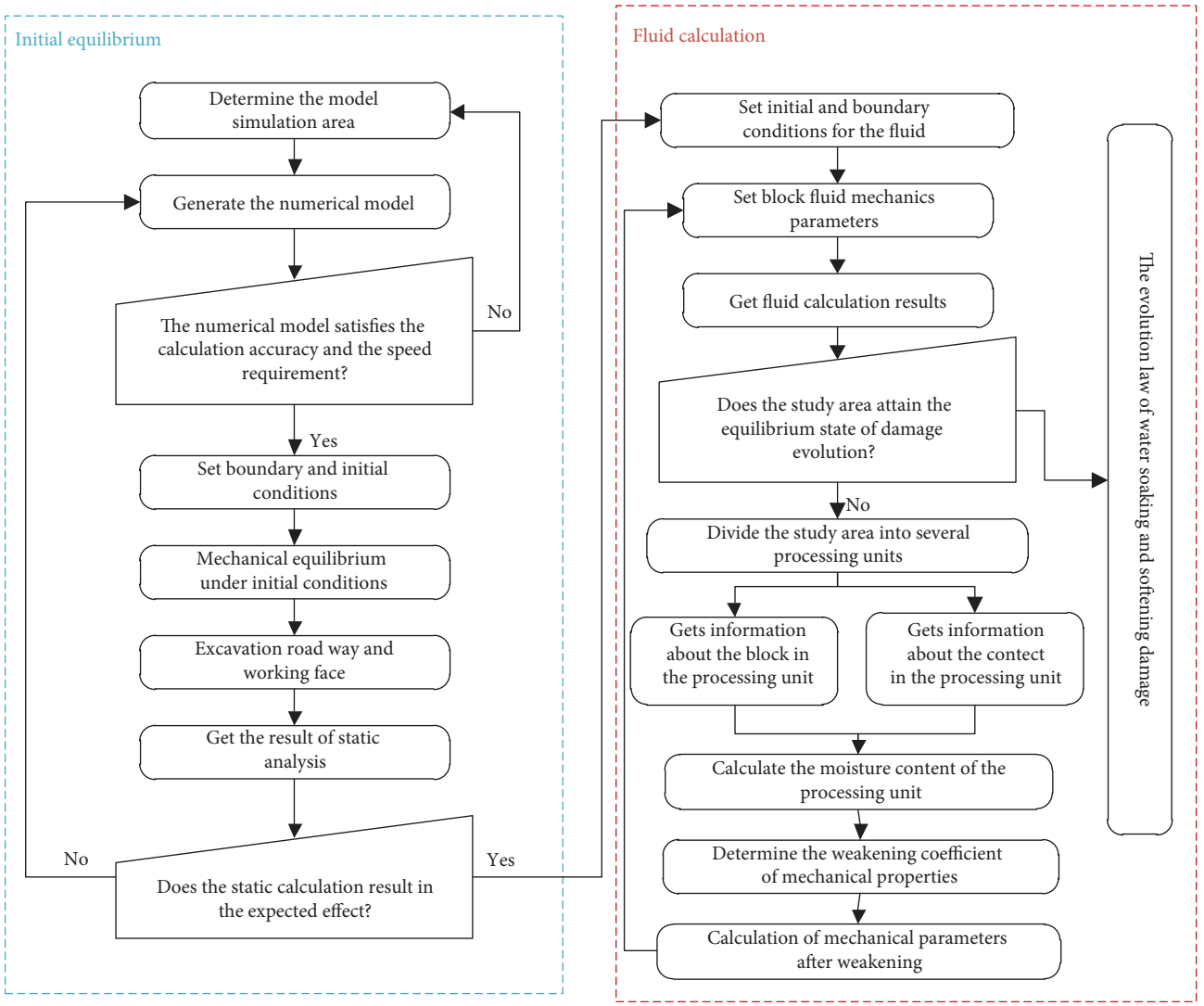

Figure 15: Flow chart for calculating mechanical properties after weakening calculation.

of the surrounding rock of the excavation space and exacerbates the degree of damage that occurs there. This can be confirmed by the fact that after water weakening treatment, the increments in the zone growth width and plastic zone width gradually decrease as the stress deepens into the coal.

5.3. Seepage Field Distribution in the Coal Pillar Dam after Water Weakening. The seepage field distribution of the coal pillar dam is shown in Figure 17.

After the water weakening treatment, the seepage pressure in the coal pillar dam was triangular and the maximum seepage width was about 10.63 m, which is 4.07 m higher than that before treatment; the maximum seepage width in the coal floor was about 13.96 m, which is 5.48 m higher than that before treatment.

As the result of water immersion, the degree of damage to the coal pillar dam was aggravated; thus, a higher number of interpenetrating fractures developed and fluid flowed into the deep coal pillar dam. The coal that was not affected by the water immersion weakened, which further reduced the effective bearing area of the coal pillar and caused the stress environment of the coal pillar to deteriorate. As a result of the deterioration of the stress environment and the reduction in the effective bearing capacity, coal pillar dam damage was

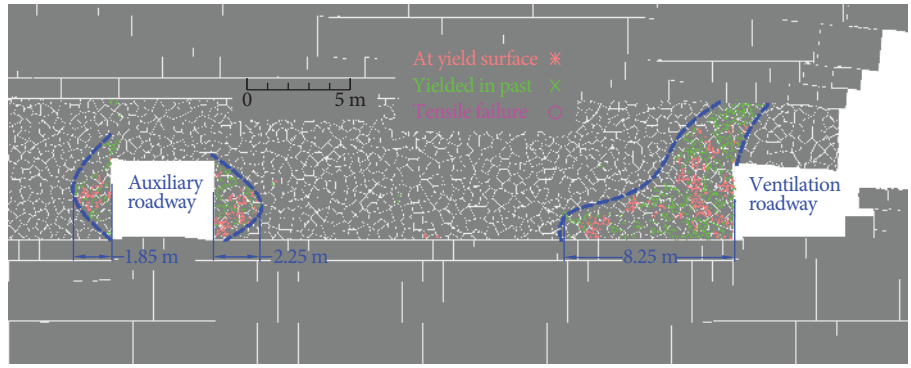

Figure 16: Distribution map of the plastic zone of the coal pillar after weakening.

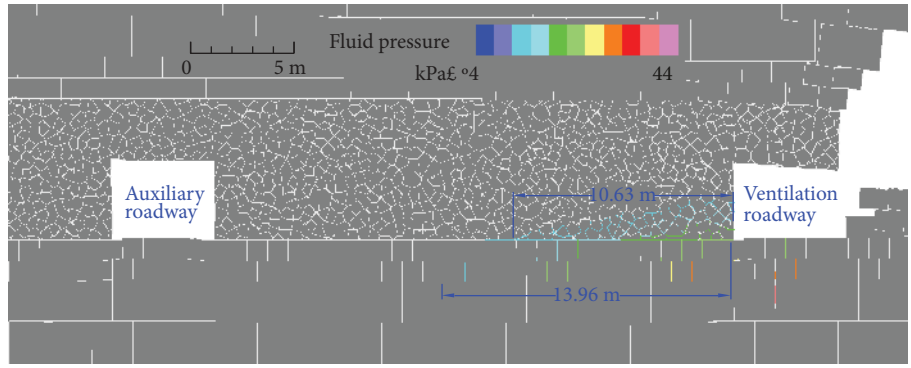

Figure 17: Seepage field distribution of the coal pillar after weakening.

intensified and the water-guiding cracks penetrated deeper into the coal pillar.

6. Conclusions

(1) An underground reservoir system is an effective means of protecting and utilizing water resources. However, the coal pillar dams required by such systems must operate in complex environments that combine dynamic-static superimposed stress fields and water immersion. Meanwhile, water immersion changes the mechanical response and deformation characteristics of the coal. A coal pillar dam under the coupling of stress and seepage is more susceptible to damage and even collapse. Therefore, the stability of coal pillar dams is a key factor in the safe and stable operation of underground reservoir systems

(2) By extracting the block and contact data in the numerical model, a method for characterizing the moisture content of the numerical simulation model was proposed for the first time. Compared with the original numerical simulation results, there were significant differences in the plastic zone depth and seepage field distribution of the coal pillar dam after a water weakening treatment. The results generated by the numerical model after the water weakening treatment were more consistent with the characteristics of coal pillar dams damaged by water immersion

(3) The seepage field of a coal pillar dam has a triangular shape. After the water weakening treatment, the maximum seepage width in the coal pillar increases from 6.56 m to 10.63 m and the maximum seepage width in the coal seam floor increases from 8.48 m to 13.96 m, resulting in respective increases of 4.07 m and 5.48 m. The plastic zone widths of the auxiliary roadways are 1.85 m and 2.25 m, and the plastic zone width of the laneway of the ventilation roadway is 8.25 m; respectively, these values are 0.21 m, 0.32 m, and 5.48 m higher than the values recorded before the water weakening treatment

(4) Owing to the distribution characteristics of the seepage field, the degree of damage to the coal pillar dam increased and more interpenetrating fissures developed, which in turn caused the seepage field to expand deep into the coal pillars. Meanwhile, the deep coal pillars that were not affected by water immersion caused further damage to the coal pillar dams, which in turn caused the seepage field to expand deep into the coal pillars. As a result, the coal that was not affected by water weakening was weakened and the degree of damage to the coal pillar dam was further aggravated

Data Availability

The data used to support the findings of this study are included within the article.

Conflicts of Interest

The authors declare no conflicts of interest.

Acknowledgments

This work was supported by the Fundamental Research Funds for the Central Universities (2018ZDPY05) and the Priority Academic Program Development of Jiangsu Higher Education Institutions. The authors gratefully acknowledge financial support from the abovementioned agencies.

References

[1] D. Z. Gu, Y. Zhang, and Z. G. Cao, "Technical progress of water resource protection and utilization by coal mining in China," *Coal Science & Technology*, vol. 44, no. 1, pp. 1–7, 2016.

[2] Z. Y. Dong and S. M. Wang, "Influence of coal exploitation on groundwater resources in Yuxi river valley of northern Shaanxi," *Journal of Arid Land Resources & Environment*, vol. 31, no. 3, pp. 185–190, 2017.

[3] S. P. Peng, *Coal Resources and Water Resources*, Beijing Science Press, 2014.

[4] Q. Wu, "Progress problems and prospects of prevention and control technology of mine water and reutilization in China," *Journal of China Coal Society*, vol. 39, no. 5, pp. 795–895, 2014.

[5] Q. Wu, J. J. Shen, and Y. Wang, "Mining techniques and engineering application for "coal-water" dual-resources mine," *Journal of China Coal Society*, vol. 42, no. 1, pp. 8–16, 2017.

[6] X. J. Qiao, G. M. Li, J. L. Zhou et al., "Analysis of influence of coal exploitation on water resources and environment: a case study of coal exploitation in Xishan of Taiyuan City," *Water Resources Protection*, vol. 26, no. 1, pp. 19–52, 2010.

[7] W. J. Chen, L. Feng, and W. Lei, "Sustainable coal mining and mining sciences," *Journal of China Coal Society*, vol. 41, no. 11, pp. 2651–2660, 2016.

[8] D. Z. Gu, "Theory framework and technological system of coal mine underground reservoir," *Journal of China Coal Society*, vol. 40, no. 2, pp. 239–246, 2015.

[9] R. L. Zhou, L. Gao, Z. Q. Guo, D. F. Cui, and J. C. Yang, "Underground direct treatment and recycle of coal mine water," *China Water & Wastewater*, vol. 29, no. 4, pp. 71–79, 2013.

[10] G. Y. Xia, "Research on resource utilization of mine water in goaf," *Coal Science & Technology*, vol. 113, no. 1, pp. 182–184, 2007.

[11] K. R. Waybrant, C. J. Ptacek, and D. W. Blowes, "Treatment of mine drainage using permeable reactive barriers: column experiments," *Environmental Science & Technology*, vol. 36, no. 6, pp. 1349–1356, 2002.

[12] W. G. Coldewey and L. Semrau, "Mine water in the Ruhr Area (Federal Republic of Germany)," in *Proceedings of Proceedings of the 5th International Mine Water Congress*, pp. 613–629, Nottingham, UK, 1994.

[13] M. Sivakumar, S. Morton, and R. N. Singh, "Case history analysis of mine water pollution in New South Wales," in *Proceedings of Proceedings of the 5th International Mine Water Congress*, pp. 823–834, Nottingham, UK, 1994.

[14] G. Hanson and A. Nilsson, "Ground-water dams for rural-water supplies in developing countries," *Groundwater*, vol. 24, no. 4, pp. 497–506, 2010.

[15] S. Ishida, T. Tsuchihara, S. Yoshimoto, and M. Imaizumi, "Sustainable use of groundwater with underground dams," *Japan Agricultural Research Quarterly*, vol. 45, no. 1, pp. 51–61, 2011.

[16] P. Bukowski, J. Wagner, and A. Witkowski, "Use of void space in abandoned mines in the Upper Silesian Coal Basin (Poland)," in *Proceedings of Proceedings of the IMWA Symposium: Water in Mining Environments*, pp. 147–151, Cagliari, Italy, 2007.

[17] Z. F. Liu, T. H. Kang, L. U. Wei, and L. Gao, "Experiment on water injection affected to mechanics features of coal body," *Coal Science & Technology*, vol. 38, no. 1, pp. 17–19, 2010.

[18] H. F. Guo, *Research of Coal and Rock Damage Weakening Under the Action of Water Pressure [Ph.D. thesis]*, Xi'an University of Science and Technology, 2010.

[19] Q. H. Niu, *Experimental Study on Shear Damage Law of Water-Bearing Coal Samples [Ph.D. thesis]*, China University of Mining and Technology, 2017.